Volume 1 | Number 1 | Jan 2013 | Pages 1–100

Journal of
Materials Chemistry A

Materials for energy and sustainability
www.rsc.org/materialsA

Li⁺

ROYAL SOCIETY
OF CHEMISTRY

ROYAL SOCIETY
OF CHEMISTRY

www.rsc.org/materialsA

Journal of Materials Chemistry A

ARTICLE

Stable organic dyes based on the benzo[1,2-b:4,5-b′]dithiophene donor for efficient dye-sensitized solar cells

Yi-Fan Chen,[a] Jun-Min Liu,[*a] Jian-Feng Huang, [a] Li-Lin Tan, [a] Yong Shen,[a] Li-Min Xiao,[b] Dai-Bin Kuang[a] and Cheng-Yong Su[*a]

Two novel nonarylamine type organic compounds (**CYF1** and **CYF2**) incorporating a substituted benzo[1,2-b:4,5-b′]dithiophene unit as the electron donor have been synthesized and used as the sensitizers of dye-sensitized solar cells (DSSCs). The relationship between the chemical structure and photovoltaic performance has been investigated. It is found that a higher molar absorption coefficient, longer electron lifetime, and larger adsorption amount are observed for sensitizer **CYF1**, which contains a single π bridge and anchoring unit, relative to **CYF2** with twin π bridges and anchoring units. As a result, under standard global AM 1.5 solar conditions, the device based on **CYF1** sensitizer gives a higher conversion efficiency of 8.02% than that based on **CYF2,** which is the highest value for amine-free organic sensitizers without any strong donor units. Moreover, the **CYF1**- and **CYF2**- sensitized DSSCs exhibit excellent stability under 1000 Wm[2] light soaking at 60 °C for 600 h. This is the first example of organic sensitizers based on benzo[1,2-b:4,5-b′]dithiophene donors for efficient dye-sensitized solar cells.

Introduction

Dye-sensitized solar cells (DSSCs) have attracted much attention after Grätzel's report in 1991 due to their low-cost fabrication and design versatility combined with high performance.[1] The sensitizer is one of the key components in DSSCs since it plays a significant role in the power conversion efficiency as well as the device stability. With great efforts, DSSCs based on zinc, ruthenium complex and pure organic dyes have reached an overall conversion efficiency of over 13%,[2] 11%,[3] and 12%,[4] respectively. Organic dyes have their unique advantages, such as tunable absorption and electrochemical properties, versatile structural modification, and lower cost than Ru complexes.

Traditionally, the most frequently used organic dyes in DSSCs are based on the arylamines or alkylamines donors.[5] We have also prepared a series of organic sensitizers with triphenylamine and carbazole donors, achieving a highest efficiency of 10% in liquid DSSCs among these dyes.[6] However, organic sensitizers using nonamine donors are still rare.[7] Very recently, we have developed a new class of nonamine dyes based on *cone*-calix[4]arene donor containing four donor-π-acceptor (D-π-A) units, the conversion efficiencies of which are effectively enhanced compared to the corresponding dyes with a single D-π-A unit.[8] To promote growth of DSSC research, novel organic dyes containing nonamine donors should been tested, which can significantly increase the choice of materials available, facilitate the understanding of DSSCs, and provide new opportunities for the development of good sensitizers. On the other hand, despite the fact amines are strong donors, they are nucleophiles and the lone pair on nitrogen increases their reactivity, resulting in the decrease of their intrinsic stability. Compared with amine-based organic sensitizers, amine-free organic sensitizers using thiophene derivatives as donors are more stable, because the delocalization of holes on the oligothiophene moieties of sensitizer may increase their photo- and chemical-stability.[5g]

In recent years there has been increasing interest in sensitizers with multiple-anchoring capability for DSSCs to increase electron extraction channels and enhance binding stability.[9] Some research groups have reported the synthesis of dyes possessing double anchors for DSSCs. The D-π-(A)$_2$ dyes have higher photocurrent but lower photovoltage than single D-π-A type dyes due to their better light harvesting but inefficient dark current suppression and/or downward shift of the titania conduction band.[9a-d] Therefore, we became interested in organic dyes using an electron-excessive moiety, which can be incorporated into muti-acceptors, as a substitute for arylamines.

The benzo[1,2-b:4,5-b′]dithiophene (BDT) unit, consisting of two thiophene rings with a benzene core, has been emerging recently as an attractive donor building block for conjugated polymers or acceptor-donor-acceptor (A-D-A) type molecules used in high performance organic solar cells (OSCs) because of their outstanding properties, which include wide absorptions with high coefficients, excellent chemical and thermal stability, and facile structural modification.[10] However, despite the extensive research into the development of OSCs based on

BDT donors, amine-free organic sensitizers using BDT as the electron donor for DSSCs, to the best of our knowledge, have not been reported, though BDT motifs were used in the spacer of arylamine-based dyes.[11]

We therefore set out to design and synthesize two novel sensitizers **CYF1** and **CYF2**, containing a 4,8-bis(5-(2-ethylhexyl)thiophen-2-yl)benzo[1,2-b:4,5-b']dithiophene donor, a 2-cyanoacrylic acid acceptor, and a 3,4'-dihexyl-2,2'-bithiophene and 3,4-ethoxythiophene (EDOT) spacer. Herein, the 4,8-positions of the BDT units were functionalized by introducing two 2-(2-ethylhexyl) thiophene groups, which incorporates the following molecular engineering concepts: (1) the thiophene groups are employed to obtain greater conjugation and thus achieve a higher short circuit current (J_{sc}); (2) the alkyl chains, 2-ethylhexyl, on the thiophene groups are introduced to enhance the solubility and suppress the aggregation of dye molecules, and thus enhance the open-circuit voltage (V_{oc}). In addition to the BDT donors, different numbers of π bridges and anchoring groups are introduced to tune interfacial electron transfer. The difference between the structures and optoelectronic properties of **CYF1** and **CYF2**, with a single and twin π bridges and anchoring groups, respectively, has been investigated by UV-vis absorption and emission spectra, cyclic voltammograms (CVs), electrochemical impedance spectroscopy (EIS), density functional theory (DFT) studies, and long-term cell stability measurement. It was found that the DSSCs based on **CYF1** exhibit both higher V_{oc} and J_{sc} compared to the DSSCs based on **CYF2**, which can be ascribed to its higher molar absorption coefficient, longer electron lifetime, and larger adsorption amount.

Experimental Section

General

^{1}H NMR spectra were recorded on a BRUKER 400 MHz spectrometer. Mass spectral data were obtained on an ultrafleX-treme MALDI-TOF/TOF mass spectrometer (Bruker Daltonics). The absorption spectra of the dyes (in solution and adsorbed on TiO_2 films) were observed with a Shimadzu UV-2450 spectrometer and fluorescence spectra were measured with a Hitachi F-4500 spectrometer. Cyclic voltammogram (CV) curves were obtained with a CHI 832 electrochemical analyzer using a normal three-electrode cell with dye-sensitized photoanode as working electrode, a Pt wire counter electrode, and a regular Ag/AgCl reference electrode in saturated KCl solution which was calibrated with ferrocene/ferrocenium as external reference. The supporting electrolyte was 0.1 M tetrabutylammonium hexafluorophosphate in THF.

Materials and reagents

Solvents were purified using MBRAUN MB SPS-800 system. Anhydrous solvents used in Suzuki coupling reaction were degassed by N_2 bubbling for 20 min. Optically transparent fluorine doped SnO_2 (FTO) conducting glass was purchased from Nippon Sheet Glass, Japan, (15 Ω/square), and cleaned by a standard procedure. All other chemicals and reagents were used as received from commercial sources without further purification. 4,8-bis(5-(2-ethylhexyl)thiophen-2-yl)benzo [1,2-b:4,5-b']dithiophene (**1**)[10f] and 7-(5'-bromo-3',4-dihexyl-[2,2'-bithiophen]-5-yl)-2,3-dihydrothieno[3,4-b][1,4]dioxine-5-carb-aldehyde (**4**)[6a] were synthesized according to the literatures.

Synthesis

7-(5'-(4,8-bis(5-(2-ethylhexyl)thiophen-2-yl)benzo[1,2-b:4,5-b']dithiophen-2-yl)-3',4-dihexyl-[2,2'-bithiophen]-5-yl)-2,3-dihydrothieno[3,4-b][1,4]dioxine-5-carbaldehyde (CYF-1-CHO). Under a nitrogen atmosphere n-butyllithium (1.6 M, 0.43 mL, 0.68 mmol) was dropwise added to THF (20 mL) solution of **1** (364 mg, 0.62 mmol) at 0 °C over 10 min. After stirring for 0.5 h, the mixture was warmed to room temperature and stirred for 1 h. Then $SnBu_3Cl$ (241 mg, 0.74 mmol) was injected into the reaction mixture at 0 °C. The reaction mixture was stirred at 0 °C for 1 h and then warmed to room temperature for 20 h. Subsequently, the reaction mixture was poured into ice water and extracted with dichloromethane. The organic phase was dried over anhydrous $MgSO_4$ and concentrated to afford the yellow crude product tributyl(8-(5-(2-ethylhexyl)thiophen-2-yl)-4-(5-(2-ethylpentyl)Thiophen-2-yl)benzo[1,2-b:4,5-b']dithiophen-2-yl)stannane (**2**) (512 mg) as a dark yellow oil.

2 (512 mg), **4** (397 mg, 0.68 mmoL), and Pd(PPh$_3$)$_4$ (35.8 mg, 0.031 mmoL) were added into the toluene (30 mL) solution in sequence under nitrogen atmosphere. After being stirred at 100 °C for 10 h, the reaction mixture was poured into cold water and extracted with ethyl acetate. The organic layer was dried over anhydrous $MgSO_4$ and concentrated to afford a dark yellow solid. The crude product was purified by silica-gel column chromatography using a mixture of chloroform and petroleum ether (3:2, v:v) as eluent to afford the product **CYF1-CHO** (401 mg) as a red solid. Yield: 60%. ^{1}H NMR (400 MHz, CDCl$_3$) δ (ppm): 9.93 (s, 1H), 7.66 (s, 1H), 7.61 (d, J = 8 Hz, 1H), 7.44 (d, J = 8 Hz, 1H), 7.31 (d, J = 8 Hz, 2H), 7.12 (s, 1H), 7.00 (s, 1H), 6.91 (t, J = 4 Hz, 2H), 4.41 (d, J = 4 Hz, 4H), 2.91-2.84 (m, 4H), 2.82-2.72 (m, 4H), 1.71-1.69 (m, 6H), 1.44-1.27 (m, 30H), 1.01-0.91 (m, 18H). ^{13}C-NMR (400 MHz, CDCl$_3$) δ (ppm): 179.8, 168.1, 148.6, 146.2, 143.5, 141.2, 139.7, 138.5, 137.8, 137.6, 137.4, 137.3, 137.2, 137.0, 135.8, 132.8, 131.2, 131.0, 129.1, 128.7, 128.6, 128.2, 128.0, 127.8, 126.6, 125.7, 124.1, 123.8, 122.7, 119.3, 116.4, 65.5,65.0 41.8, 39.0, 34.6, 32.8, 32.0, 31.9, 30.7,30.6, 30.4, 30.0, 29.6, 29.2, 26.1,26.0, 24.0, 23.3,22.9, 14.5, 14.3, 11.3. MALDI-TOF: *m/z* 1078.453 ([M]$^+$).

(E)-3-(7-(5'-(4,8-bis(5-(2-ethylhexyl)thiophen-2-yl)benzo[1,2-b:4,5-b']dithiophen-2-yl)-3',4-dihexyl-[2,2'-bithiophen]-5-yl)-2,3-dihydrothieno[3,4-b][1,4]dioxin-5-yl)-2-cyanoacry-lic acid (CYF-1). Under a nitrogen atmosphere, **CYF1-CHO** (208 mg, 0.192 mmol) and cyanoacetic acid (86.8 mg, 1.04 mmoL) were added into a 100 mL Schlenk flask, and then acetonitrile (20 mL), toluene (10 mL), and piperidine (164 mg, 1.92 mmoL) were added to the reaction mixture. After being stirred for 8 h at 85 °C, the reaction mixture was adjusted to PH = 2~3 with 1 M aqueous HCl, and then extracted with chloroform. The organic phase was dried over anhydrous $MgSO_4$ and evaporated to afford a dark red solid. The crude product was further purified by silica-gel column chromatography using a mixture of chloroform, petroleum ether, and acetic acid (1:1:1.6×10^{-4}, v:v:v) as eluent to afford **CYF1** 198 mg as a dark red solid. Yield: 90%. ^{1}H NMR (400 MHz, CDCl$_3$) δ (ppm): 8.27 (s, 1H), 7.63 (s, 1H), 7.57 (d, J = 8 Hz, 1H), 7.39 (d, J = 8 Hz, 1H), 7.33 (d, J = 4 Hz, 1H), 7.09 (s, 1H), 6.97 (s, 1H), 6.94 (d, J = 4 Hz, 1H), 6.89 (d, J = 4 Hz, 1H), 4.40 (d, J = 20 Hz, 4H), 2.91-2.86 (m, 4H), 2.83-2.73 (m, 4H), 2.11-2.03 (m, 6H), 1.72-1.66 (m, 4H), 1.45-1.35 (m, 24H), 0.99-0.92 (m, 18H). ^{13}C-NMR (400 MHz, THF-d_8) δ (ppm): 164.2, 148.5, 146.3, 143.8, 141.6, 140.4, 140.2, 138.6, 138.3, 138.1, 137.7, 137.6, 137.5, 137.3, 135.8, 131.5, 130.2, 129.3, 129.1, 128.6, 128.5, 127.6, 126.2, 124.4, 124.2, 123.6, 121.5, 119.2, 116.8,

2 | *J. Mater. Chem. A*, 2015, **00**, 1-3

This journal is © The Royal Society of Chemistry 2013

111.2, 66.3, 65.6, 42.2, 34.6, 33.1, 32.5, 32.4, 32.3, 31.2, 30.9, 30.8, 30.3, 30.2, 30.1, 29.9, 29.5, 27.7, 26.3, 23.6, 23.2, 14.2, 14.1, 11.0, 10.9. MALDI-TOF: m/z 1145.362. ([M]$^+$).

7,7'-(5',5'''-(4,8-bis(5-(2-ethylhexyl)thiophen-2-yl)benzo[1,2-b:4,5-b']dithiophene-2,6-diyl)bis(3',4-dihexyl-[2,2'-bithiophene]-5',5-diyl))bis(2,3-dihydrothieno[3,4-b][1,4]dioxine-5-carbaldehyde) (CYF-2-CHO). Under a nitrogen atmosphere n-butyllithium (1.6 M, 0.98 mL, 1.56 mmol) was dropwise added to the THF (25 mL) solution of **1** (347 mg, 0.60 mmol) at 0 °C over 10 min. After stirring for 0.5 h, the mixture was warmed to room temperature and stirred for 1 h. Then SnBu$_3$Cl (547 mg, 1.68 mmol, 0.46 mL) was added into the reaction mixture at 0 °C. The reaction mixture was stirred for 1 h and then warmed to room temperature for 20 h. Subsequently, the reaction mixture was poured into ice water and extracted with dichloromethane. The organic phase was dried over anhydrous MgSO$_4$ and concentrated to afford the crude product (4-(5-(2-ethylhexyl)thiophen-2-yl)-8-(5-(2-ethylpentyl)thiophen-2-yl)benzo[1,2-b:4,5-b']dithiophene-2,6-diyl)bis(tributylstannane) (**3**) (624 mg) as a red oil.

The mixture of **3** (624 mg), **4** (872 mg, 1.5 mmol) and Pd(PPh$_3$)$_4$ (69.3 mg, 0.06 mmol) was added into toluene (30 mL) under nitrogen atmosphere. The mixture was stirred for 24 h at 110 °C,   and then extracted with acetic ether and washed with water. The organic content was dried over anhydrous MgSO$_4$, concentrated and further purified by silica-gel column chromatography using the mixture of chloroform and petroleum ether (2:1, v:v) as eluent to afford the product **CYF2-CHO** (710 mg) as a red solid. Yield: 75%. ^{1}H NMR (400 MHz, CDCl$_3$) δ (ppm): 9.94 (s, 2H), 7.61 (s, 2H), 7.31 (d, J = 4 Hz, 2H), 7.11 (s, 2H), 7.00 (s, 2H), 6.99 (s, 1H), 6.94 (d, J = 4 Hz, 2H), 4.42 (d, J = 4 Hz, 8H), 2.90-2.89 (d, J = 4 Hz, 2H), 2.82-2.73 (m, 10H), 1.69-1.63 (m, 14H), 1.40-1.32 (m, 36H), 0.99-0.88 (m, 24H). ^{13}C-NMR (400 MHz, CDCl$_3$) δ (ppm): 179.7, 148.4, 146.2, 143.4, 141.1, 138.9, 137.7, 137.6, 137.5, 137.0, 135.6, 130.9, 128.6, 128.4, 128.0, 126.6, 125.7, 123.5, 122.6, 119.2, 116.3, 65.4, 64.9, 41.7, 34.5,32.7, 31.9, 31.8, 30.6, 30.5, 29.9, 29.8, 29.5, 29.1, 26.0, 23.3, 22.8, 14.4, 14.3, 11.2. MALDI-TOF: m/z 1577.540. ([M]$^+$).

(2E,2'E)-3,3'-(7,7'-(5',5'''-(4,8-bis(5-(2-ethylhexyl)thiophen-2-yl)benzo[1,2-b:4,5-b']dithiophene-2,6-diyl)bis(3',4-dihexyl-[2,2'-bithiophene]-5',5-diyl))bis(2,3-dihydrothieno[3,4-b][1,4]dioxine-7,5-diyl))bis(2-cyanoacrylic acid) (CYF-2) Under a nitrogen atmosphere, **CYF2-CHO** (130 mg, 0.086 mmol) and cyanoacetic acid (72.8 mg, 0.86 mmol) were added into a 100 mL Schlenk flask, and then acetonitrile (20 mL), toluene(10 mL), and piperidine (148 mg, 1.74 mmol) were added to the reaction mixture. After being stirred for 10 h at 85 °C, the reaction mixture was adjusted to PH = 2~3 with 1M aqueous HCl, and then extracted with chloroform. The organic phase was dried over anhydrous MgSO$_4$ and evaporated to afford a dark red solid. The crude product was further purified by silica-gel column chromatography using a mixture of tetrahydrofuran, chloroform, and acetic acid (1.5:1:1.8×10^{-4}, v:v:v) as eluent to afford **CYF2** 127 mg as a dark red solid. Yield: 86%. ^{1}H NMR (400 MHz, THF-d_8) δ (ppm): 8.33 (s, 2H), 7.66 (s, 2H), 7.37 (d, J = 4 Hz, 2H), 7.28 (s, 2H), 7.14 (s, 2H), 7.00 (d, J = 4 Hz, 2H), 4.46-4.42 (m, 8H), 2.95-2.87 (m, 8H), 2.84-2.81 (m, 4H), 1.48-1.35 (m, 50H), 1.01-0.88 (m, 24H). ^{13}C-NMR (400 MHz, THF-d_8) δ (ppm): 171.3, 152.9, 152.7, 149.0, 148.0,147.6, 146.3, 143.3, 142.5, 142.1, 141.3, 138.3, 138.1, 133.8, 133.5, 128.8, 127.2, 125.9, 125.4, 125.1, 78.4, 45.5, 39.3, 35.4,35.2, 35.1, 30.8, 30.7, 29.8, 28.6, 21.4,14.4. MALDI-TOF: m/z 1714.732. ([M]$^+$).

Fabrication of Cells

The anatase TiO$_2$ nanoparticles were synthesized according to our previous literature.[12] First, the Ti(OBu)$_4$ (10 mL) was added to the ethanol (20 mL) under stirring for 10 min. Then a mixture of deionized water (50 mL) and acetic acid (18 mL) was added to the solution with vigorous stirring for 1 h. The solution was moved to an autoclave and heated at 200 °C for 12 h. Finally, the precipitations were washed with deionized water and ethanol for several times, respectively. The white powder was obtained after drying in air. The as-prepared TiO$_2$ nanoparticles were anatase crystals with diameters of about 20 nm, as confirmed by SEM, TEM, and XRD. The prepared TiO$_2$ powder (1.0 g) was ground for 40 min in the mixture of acetic acid (0.2 mL), ethanol (8.0 mL), ethyl cellulose (0.5 g), and terpineol (3.0 g) to form a slurry, and then the slurry was sonicated for 5 min to obtained a viscous white TiO$_2$ paste. The TiO$_2$ paste was then screen-printed onto the surface of FTO coated glass forming photoanode film. The thickness of films can be easily controlled through repeating screen-printing times. Afterwards, a programmed heating process was carried out to remove the organic substances in the film. The as-prepared TiO$_2$ films (~15 μm) were soaked in a 0.04 M aqueous solution of TiCl$_4$ for 30 min at 70 °C and then sintered at 520 °C for 30 min. After cooling to 80 °C, the TiO$_2$ electrodes were immersed into 0.3 mM optimal organic solution (CHCl$_3$/ACN/^{t}BuOH = 1/2/2, v:v:v) of the dyes and kept at room temperature for 6 h for cells with liquid electrolyte and for 12 h for cells with gel electrolyte, respectively. And then the prepared TiO$_2$ working electrodes were sandwiched together with Pt-counter electrode. The active area of the dye-coated TiO$_2$ film was 0.16 cm^2. The electrolyte was injected into the inter-electrode space. The electrolyte solution is composed of 0.6 M 1-methyl-3-propylimidazolium iodine (PMII), 0.03 M I$_2$, 0.05 M LiI, 0.1 M guanidinium thiocyanate (GuSCN), and 0.5 M 4-tert-butylpyridine (TBP) in acetonitrile and valeronitrile (85:15, v:v).

Characterization of Cells

The TiO$_2$ film thickness and active area of the dye-coated TiO$_2$ film was measured by using a profilometer (Ambios, XP-1). The current-density voltage (*J-V*) curves of the DSSCs were recorded by using a Keithley 2400 source meter under the illumination of AM 1.5 G simulated solar light. The incident photon-to-current conversion efficiencies (IPCEs) of DSSCs were measured on the basis of a Spectral Products DK240 monochromator. Electrochemical impedance spectroscopy (EIS) was measured using an electrochemical workstation (Zahner, Zennium) with a frequency response analyzer at a bias potential of -800 mV in the dark with a frequency ranging from 10 mHz to 1 MHz. The dye-adsorbed amounts on the TiO$_2$ film were measured using a Shimadzu UV-2450 spectrometer. Intensity modulated photocurrent spectroscopy (IMPS) and intensity modulated photovoltage spectroscopy (IMVS) measurements were conducted using electrochemical workstation (ZAHNER, Zennium) and were performed under a modulated LED light (457 nm) driven by a source supply (ZAHNER, PP210). The illumination intensity ranged from 30 to 150 mW cm^{-2}. The light intensity modulation was 20% of the base light intensity over the frequency range of 10^{-1}-10^3 Hz.

Results and discussion

Synthesis

This journal is © The Royal Society of Chemistry 2013

J. Mater. Chem. A, 2015, **00**, 1-3 | **3**
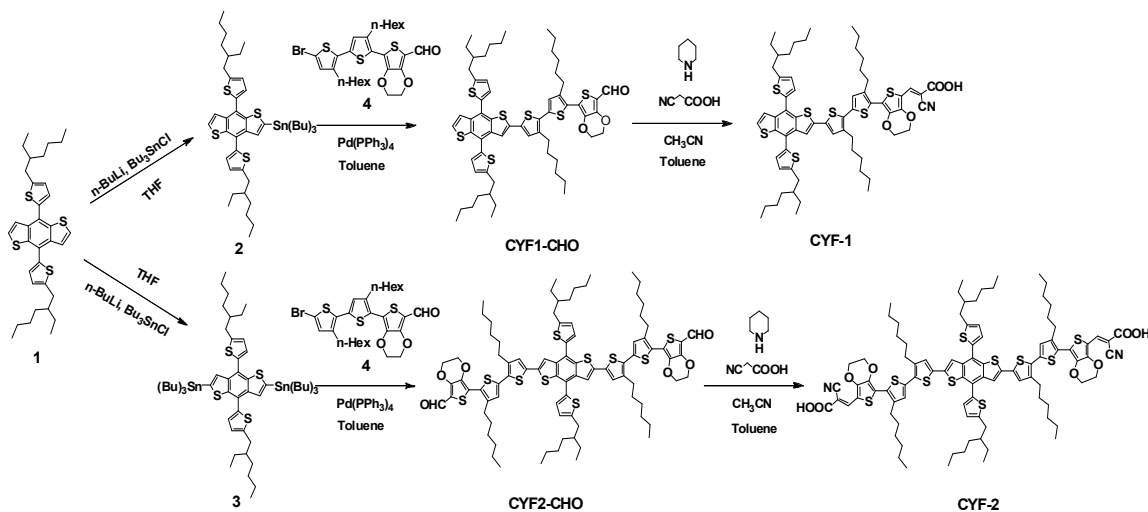
Scheme 1 synthesis of **CYF1** and **CYF2**

The synthesis of sensitizers **CYF1** and **CYF2** is shown in Scheme 1. The starting material **1**, *i.e.* 4,8-bis(5-(2-ethylhexyl)thiophen-2-yl)benzo[1,2-b:4,5-b'] dithiophene, coupled with 1 and 2 equivalents of $SnBu_3Cl$ through stille coupling reaction to afford **2** and **3**, respectively. Then, **2** reacted with 1 equivalent of **4** (or **3** reacted with 2 equivalents of **4**) in the presence of $Pd(PPh_3)_4$ to generate **CYF1-CHO** (or **CYF2-CHO**). Finally, **CYF1** and **CYF2** were obtained from **CYF1-CHO** and **CYF2-CHO**, respectively, *via* a Knoevenagel condsensation with cyanoacetic acid by refluxing in acetonitrile in the presence of piperidine. The chemical structures of these new compounds have been verified using ^{1}HNMR, ^{13}CNMR spectroscopy, and mass spectroscopy.

UV-vis absorption properties

The UV-vis absorption spectra of sensitizers **CYF1** and **CYF2** in THF solution are depicted in Fig. 1a, and the corresponding data are summarized in Table 1. **CYF1** and **CYF2** exhibit two major absorption bands in the range of 300-600 nm. The band below 400 nm corresponds to the π-π* transition and the other band at 450-550 nm can be assigned to the intramolecular charge transfer (ICT) from the donor unit to the cyanoacrylic acid acceptor moiety to produce an efficient charge-separated state. The λ_{max} at ICT band of **CYF2** red-shifts about 17 nm from the **CYF1** because of the longer conjugated π-chromophore in **CYF2**. However, the molar extinction coefficients of **CYF1** at π-π* band are much higher than those of **CYF2**, and its ICT absorption band is also more intense relative to **CYF2**, which indicates that stronger ICT interactions occur in **CYF1**, in agreement with the report in other ICT systems with increased number of electron-withdrawing group.[13] This can be explained by the disperse of the electron push-pull effect resulting from two competing anchoring groups in sensitizer **CYF2**.

The absorption spectra of organic sensitizers **CYF1** and **CYF2** on the TiO_2 films are shown in Fig. 1b. Extension of **CYF1** and **CYF2** spectra beyond 600 nm implies the existence of *J*-aggregation of dye molecules on the TiO_2 surface.[9f] The ICT band of the **CYF1**-loaded TiO_2 film displays no obvious shift in comparison to that in THF, indicating the ICT from the BDT donor to the acceptor was not weaken despite the anchoring group being deprotonated. By contrast, the ICT band for **CYF2** exhibits only unresolved shoulders at around 500 nm, probably due to the absorption band overlapping. A slight

hypsochromic shift of the absorption maximum of **CYF2** occurs when compared with that dissolved in THF, which could be ascribed to the deprotonation of the twin anchoring groups.
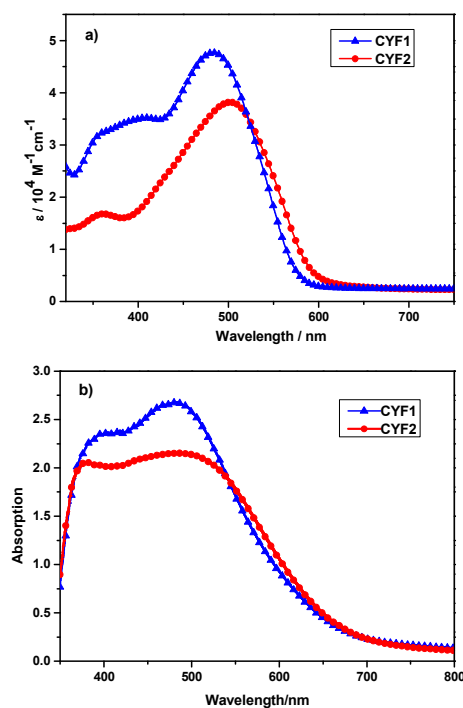

Fig. 1 Absorption spectra of **CYF1** and **CYF2** (a) in THF solution and (b) on TiO_2.

Molecular orbital calculations

The electronic structure calculations of **CYF1** and **CYF2** were carried out using the TD-DFT and B3LYP-3-21G* program. All dihedral angles between the thiophene planes in **CYF1** and **CYF2** dyes are listed in Table S1. The angles between BDT and 2-(2-ethylhexyl) thiophene plane in **CYF1** (A1-A2) and **CYF2** (B1-B2) are as large as 53.2° and 53.5°, respectively, which can prevent π-π aggregation of dye. On the other hand, the coplanarity between the DBT donor and the close bridging thiophene ring in **CYF1** (A1-A3) and **CYF2** (B1-B3) dyes is

Table 1. Absorption and electrochemical data of the dyes

dye	$\varepsilon/10^4 M^{-1} cm^{-1}$ (λ_{max}/nm)	[a]E_{ox}/V (*vs.* Fc/Fc$^+$)	[b]E_{0-0}/eV	[c]E_{HOMO}/eV (*vs.* vacuum)	[d]E_{LUMO}/eV (*vs.* vacuum)	amounts/ 10^{-6} mol cm^{-2}
CYF1	3.82 (501)	0.35	2.23	-5.15	-2.92	4.15
CYF2	4.77 (484)	0.45	2.16	-5.25	-3.09	2.09

[a] The Ag/AgCl reference electrode was calibrated using Fc/Fc$^+$. [b] E_{0-0} was determined from the intersection of absorption and emission spectra in THF. [c] E_{HOMO} [eV] $= - (E_{ox}$ (vs Fc/Fc$^+$) + 4.8). [d] E_{LUMO} [eV] $= E_{HOMO} + E_{0-0}$.

distinct, as verified by the 9.2° and 9.7° of the dihedral angles, respectively, which may favor the electron transport process.

The calculated molecular orbitals of **CYF1** and **CYF2** with isodensity plots of the highest occupied molecular orbital (HOMO) and lowest unoccupied molecular orbital (LUMO) are illustrated in Fig. 2. The HOMOs of **CYF1** and **CYF2** are delocalized on the donor groups and extend to the π bridges, whereas the LUMOs of these molecules are concentrated on the cyanoacrylic moieties. It was expected that the LUMOs of **CYF2** are stretched out to two-anchoring parts of carboxylic groups. As a result, the HOMO-LUMO excitation could transfer the electron distribution from the DBT donor to the cyanoarylic acid moiety through the π-conjugation bridge.
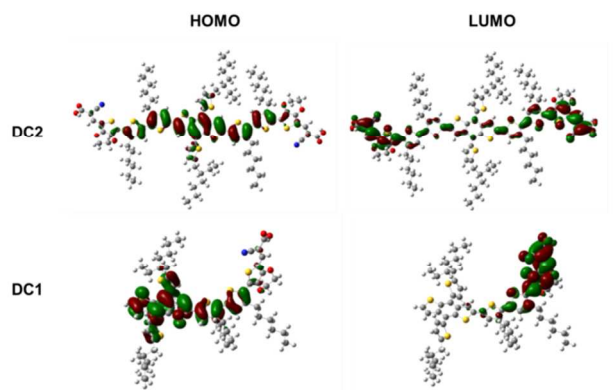
Fig. 2 Frontier molecular orbitals (HOMO and LUMO) of **CYF1** and **CYF2** calculated with DFT on the B3LYP/6-31G* level.

Electrochemical properties

The electrochemical properties of the sensitizers were measured using cyclic voltammetry (CV) in CH$_2$Cl$_2$ and their electrochemical data were listed in Table 1.[14] The first oxidation potentials, corresponding to the HOMO energy levels of sensitizers **CYF1** and **CYF2**, were determined to be -5.15 and -5.25 eV, respectively, which are more positive than the I$^-$/I$_3^-$ redox couple (-4.9 eV), providing a thermodynamic driving force for efficient dye regeneration. Accordingly, the LUMO energy levels of dyes **CYF1** and **CYF2**, estimated from the oxidation potentials and absorption/emission data, were calculated to be -2.92 and -3.09 eV, which are more negative than the conduction edge of the TiO$_2$ (-3.9 eV),[15] indicating that the electron injection process is energetically permitted. Although the electron donating group, π-conjugated bridge, and electron acceptor of the two sensitizers are identical, the difference of the energy levels can be traced to the diverse number of π-conjugated and anchoring groups.

Photovoltaic properties

The photovoltaic performance of **CYF1-** and **CYF2-**sensitized solar cells with liquid electrolyte is shown in Fig. 3a. The J_{sc}, V_{oc}, and FF values for the **CYF1** based DSSC are 17.87 mA cm^{-2}, 683 mV, and 0.66, respectively, which corresponds to a η of 8.01%. To the best of our knowledge, this is the first time such a high efficiency has been obtained for liquid-based DSSCs with amine-free organic sensitizers. Under the same conditions, the DSSC based on **CYF2**, which has two anchoring units, features J_{sc}, V_{oc}, FF, and η values of 14.64 mA cm^{-2}, 592 mV, 0.68, and 5.85%, respectively. The superior performance of sensitizer **CYF1** relative to **CYF2** is particularly noteworthy.

To elucidate the difference between the J_{sc} values, the incident photon-to-current conversion efficiencies (IPCEs) for the DSSCs based on sensitizers **CYF1** and **CYF2** are shown in Fig. 3b. All cells tested can convert the light to photocurrents in the wide wavelength region up to about 750 nm. The IPCE spectrum of the cell based on **CYF1** exhibits a plateau between 420 and 590 nm with an IPCE value of over 80%, while **CYF2** based cell displays an IPCE spectrum with a similar spectral pattern, but with decreased intensity and maximum. The result agrees well with the trends in their absorption spectra both in solution and on the TiO$_2$ film. Consequently, the increase of J_{sc} values for sensitizer **CYF1** compared with **CYF2** could be attributed to its wider IPCE spectra and better dye adsorption (Table 1).

This journal is © The Royal Society of Chemistry 2013

*J. Mater. Chem. A*, 2015, **00**, 1-3 | **5**
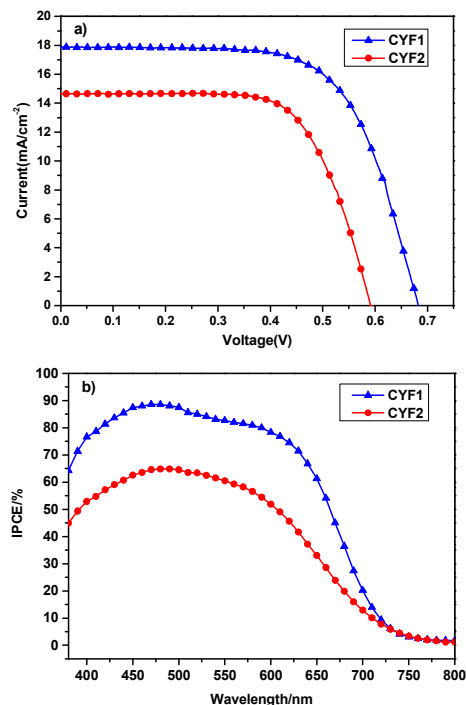
Fig. 3 (a) Photocurrent density *vs.* voltage and (b) incident photon-to-current conversion efficiency spectra for DSSCs based on **CYF1** and **CYF2** under AM 1.5 G simulated solar light (100 mW cm^2).

Electrochemical impedance spectroscopy (EIS) analysis was performed to explain the different V_{oc} values obtained for the DSSCs based on **CYF1** and **CYF2**.[16] The second semicircle (R$_{rec}$) in the Nyquist plot is attributed to charge transfer at the TiO$_2$/dye/electrolyte interface. Obviously, a larger R$_{rec}$ indicates a slower charge recombination, smaller dark current, and higher V_{oc}. Fig. 4a shows the radius of the second semicircle of **CYF1** is larger than that of **CYF2**, implying its electron recombination resistance is higher than **CYF2**. Electron lifetmes (τ) obtained from curve fitting is 184.1 and 81.8 ms for **CYF1** and **CYF2**, respectively, which corresponds well with the V_{oc} values obtained in *J-V* curves. Though **CYF1** and **CYF2** have similar chemical structures, the V_{oc} values are greatly affected by the number of the π-conjugated bridges and anchoring groups. The observation indicates that introduction of two π-conjugated bridges and anchoring units does not improve the V_{oc}. We deduce the cell based on **CYF2** gives the lower V_{oc} value due to the two factors: (1) the extra protons released from the D-(π)$_2$-(A)$_2$ molecules will lower the Fermi level of TiO$_2$, leading to the V_{oc} decrease; (2) the lower dye loading leaves more void space for electrolyte penetration, resulting in a larger dark current. The Bode phase plots (Fig. 4b) show the middle-frequency peak of the cell based on **CYF1** shifts to a lower frequency relative to **CYF2**, displaying a longer lifetime for **CYF1**, supporting the difference in the electron lifetime for TiO$_2$ film derivatized with the two sensitizers.
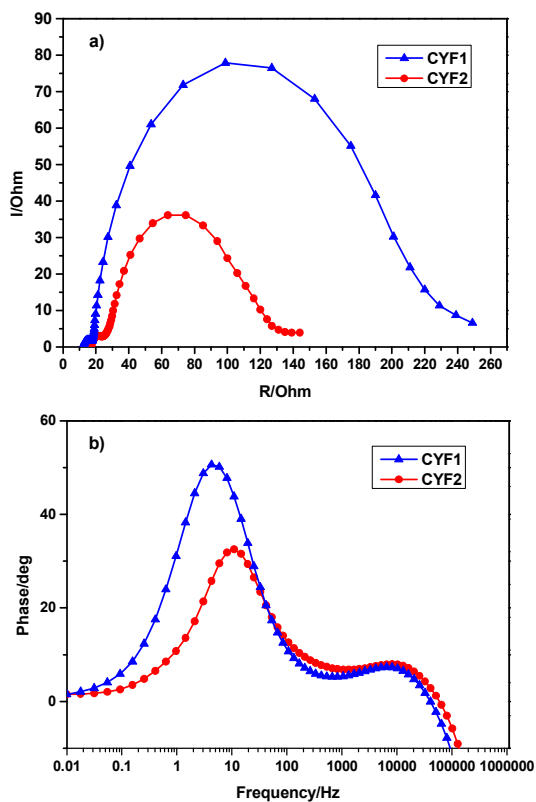
Fig. 4 (a) EIS Nyquist plots (i.e. minus imaginary part of the impedance –Z'' vs. the real part of the impedance Z' when sweeping the frequency) and (b) EIS Bode plots (i.e. the impedance -Z'' vs. the frequency) for DSSCs based on **CYF1** and **CYF2** sensitizers.

To further confirm the different photovoltaic behaviors of two sensitizers, intensity modulated photocurrent spectroscopy (IMPS) and intensity modulated photovoltage spectroscopy (IMVS) were performed. As shown in Fig. 5a, the recombination time ($τ_r$) of DSSCs based on **CYF1** sensitizers under various incident light intensities is longer than that based on **CYF2**, consistent with the EIS results described above. On the other hand, Fig. 5b shows the electron transport time ($τ_d$) of DSSCs based on **CYF1** sensitizers is shorter than that of **CYF2**. It is known that the adsorption of Li$^+$ in the TiO$_2$ electrodes increases the local cation density and assists the electron diffusion along the TiO$_2$ network.[17] Therefore, we speculate that the more protons released from the **CYF2** sensitizers with twin carboxyl groups might limit the access of Li$^+$ to the TiO$_2$ surface due to electrostatic repulsion, and thus prolong the electron transport time.
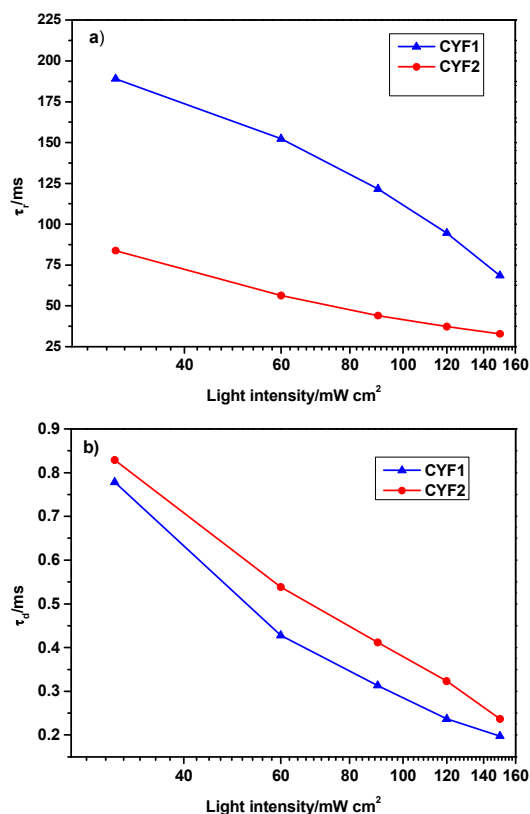
Fig. 5 (a) Incident light intensity dependent recombination time constants, and (b) incident light intensity dependent transport time constants for DSSCs based on **CYF1** and **CYF2** sensitizers.

Long-term stability

The long-term stability of DSSCs based on **CYF1** and **CYF2** was measured under AM 1.5 light for at least 600 h, as shown in Fig. 6. After 1000 h light soaking, the V_{oc} of **CYF1** based cells decreases by 67 mV and the *FF* declines from 0.68 to 0.66, but the J_{sc} increases by 1.05 mA cm^{-2}. As a consequence, the efficiency decreases from 7.48% to 7.04 % and remains at 94% of the initial value. The cells based on **CYF2** were also subjected to testing under the same conditions. The V_{oc} value decreases by 66 mV and the *FF* remains constant, but the J_{sc} increases by 1.39 mA cm^{-2}. And thus the overall efficiency remains at 95% (4.75%) of the initial value (5.00%). The results demonstrate that the **CYF1** and **CYF2** sensitizers sustain without noticeable decline in performance.[18]
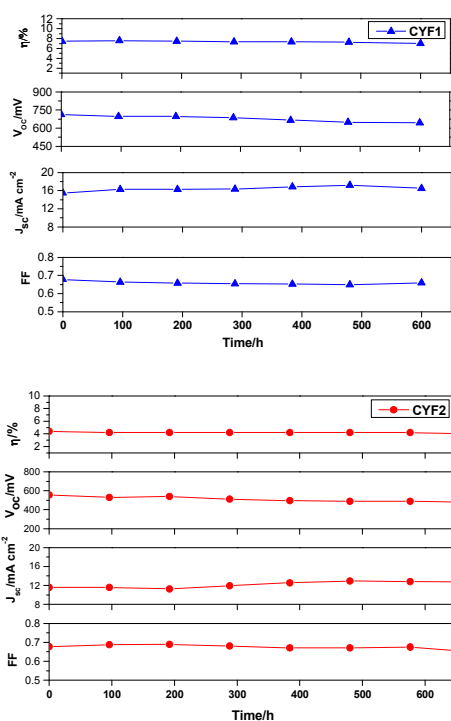
Fig. 6 Variations of photovoltaic parameters (η, J_{sc}, V_{oc}, and FF) with aging time for DSSC devices based on **CYF1** and **CYF2** under AM 1.5 light soaking at 60 ^{o}C.

Conclusions

In summary, two novel amine-free organic sensitizers based on BDP donor, **CYF1** and **CYF2**, with a single and twin π bridges and anchoring groups, respectively, have successfully synthesized and applied in DSSCs. The cell based on **CYF1** gives an improved conversion efficiency of 8.08%, compared to **CYF2**, which can be due to higher molar absorption coefficients, longer electron lifetimes, and larger adsorption amounts. To the best of our knowledge, this is the first time such a high efficiency has been obtained for liquid DSSCs with amine-free organic sensitizers without any strong donor units. Moreover, the **CYF1** and **CYF2** sensitizers containing BDP donors show excellent stability, which remain at 94% and 95% of the initial value under 100 mW cm^{-2} light soaking at 60 °C for 500 h, respectively. We believe that the use of BDP as a donor in organic sensitizers presents new opportunities for the development of efficient amine-free organic sensitizers.

Acknowledgements

Notes and references

a MOE Laboratory of Bioinorganic and Synthetic Chemistry/KLGHEI of Environment and Energy Chemistry, State Key Laboratory of Optoelectronic Materials and Technologies, School of Chemistry and Chemical Engineering, Sun Yat-Sen University, Guangzhou, 510275, China. E-mail: liujunm@mail.sysu.edu.cn;cesscy@mail.sysu.edu.cn; Fax:+86-20-84115178; Tel: +86-20-84115178.

b School of Computer Science and Engineering, Beihang University, Beijing, 100191, China.

Electronic Supplementary Information (ESI) available: Cyclic voltammograms of the two sensitizers. The dihedral angles between the phenyl planes and thiophene units in the two sensitizers. See DOI: 10.1039/b000000x/

1   (a) B. O'Regan and M. Grätzel, *Nature*, 1991, **353**, 737; (b) A. Hagfeldt and M. Grätzel, *Acc Chem Res*, 2000, **33**, 269; (c) M. Grätzel, *Nature*, 2001, **414**, 338.

2   S. Mathew, A. Yella, P. Gao, R. Humphry-Baker, B. F. E. Curchod, N. Ashari-Astani, I. Tavernelli, U. Rothlisberger, M. K. Nazeeruddin and M. Grätzel, *Nature Chem.*, 2014, **6**, 242.

3   J.-H. Yum, I. Jung, C. Baik, J. Ko, M. K. Nazeeruddin and M. Grätzel, Energy Environ. Sci., 2009, 2, 100.

4   K. Kakiage, Y. Aoyama, T. Yano, T. Otsuka, T. Kyomen, M. Unno and M. Hanaya, *Chem. Commun.*, 2014, **50**, 6379.

5   (a) S. Ahmad, E. Guillèn, L. Kavan, M. Grätzel and M. K. Nazeeruddin, *Energy Environ. Sci.*, 2013, **6**, 3439; (b) M. Liang and J. Chen, *Chem. Soc. Rev.,* 2013, **42**, 3453; (c) A. Hagfeldt, G. Boschloo, L. Sun, L. Kloo and H. Pettersson, *Chem. Rev.* 2010, **110***, 6595; (e) J. Yang, P. Ganesan, J. Teuscher, T. Moehl, Y. J. Kim, C. Yi, P. Comte, K. Pei, T. W. Holcombe, M. K. Nazeeruddin, J. Hua, S. M. Zakeeruddin, H. Tian and M. Grätzel, *J. Am. Chem. Soc*, 2014, **136**, 5722; (f) Z. Ning, Y. Fu and H. Tian, *Energy Environ. Sci.*, 2010, **3**, 1170; (g) R. Katoh, A. Furube, S. Mori, M. Miyashita, K. Sunahara, N. Koumura and K. Hara, *Energy Environ. Sci.*, 2009, **2**, 542.

6   (a) L.-L. Tan, J.-F. Huang, Y. Shen, L.-M. Xiao, J.-M. Liu, D.-B. Kuang and C.-Y. Su, *J. Mater. Chem. A*, 2014, **2**, 8988; (b) L.-L. Tan, H.-Y. Chen, L.-F. Hao, Y. Shen, L.-M. Xiao, J.-M. Liu, D.-B. Kuang and C.-Y. Su, *Phys. Chem. Chem. Phys.*, 2013, **15**, 11909; (c) J.-F. Huang, J.-M. Liu, L.-L. Tan, Y.-F. Chen, Y. Shen, L.-M. Xiao, D.-B. Kuang and C.-Y. Su, *Dyes Pigm.*, 2015, **114**, 18; (d) L.-L. Tan, L.-J. Xie, Y. Shen, J.-M. Liu, L.-M. Xiao, D.-B. Kuang and C.-Y. Su, *Dyes Pigm.*, 2014, **100**, 269.

7   (a) H.-Y. Yang, Y.-S. Yen, Y.-C Hsu, H.-H. Chou and J. T. Lin, *Org. Lett.*, 2010, **12**, 16; (b) Y. Kubo, D. Eguchi, A. Matsumoto, R. Nishiyabu, H. Yakushiji, K. Shigaki and M. Kaneko, *J. Mater. Chem. A*, 2014, **2**, 5204; (c) S. Tan, J. Zhai, H. Fang, T. Jiu, J. Ge, Y. Li, L. Jiang and D. Zhu, *Chem. Eur. J.*, 2005, **11**, 6272.

8   L.-L. Tan, J.-M. Liu, S.-Y. Li, L.-M. Xiao, D.-B. Kuang and C.-Y. Su, 2015, **8**, 280.

9   (a) A. Abbotto, N. Manfredi, C. Marinzi, F. D. Angelis, E. Mosconi, J.-H. Yum, Z. Xianxi, M. K. Nazeeruddin and M. Grtäzel, *Energy Environ. Sci.*, 2009, **2**, 1094; (b) X. Jiang, K. M. Karlsson, E. Gabrielsson, E. M. J. Johansson, M. Quintana, M. Karlsson, L. Sun, G. Boschloo and A. Hagfeldt, *Adv. Funct. Mater.*, 2011, **21**, 2944; (c) J. Liu, J. Zhang, M. Xu, D. Zhou, X. Jing and P. Wang, *Energy Environ. Sci.*, 2011, **4**, 3021; (d) X. Lu, X. Jia, Z.-S. Wang and G. Zhou, *J. Mater. Chem. A*, 2013, **1**, 9697; (e) S. Jiang, S. Fan, X. Lu, G. Zhou and Z.-S. Wang, *J. Mater. Chem. A*, 2014, **2**, 17153; (f) R. Y.-Y. Lin, F.-L. Wu, C.-H. Chang, H.-H. Chou, T.-M. Chuang, T.-C. Chu, C.-Y. Hsu, P.-W. Chen, K.-C. Ho, Y.-H. Loc and J. T. Lin, *J. Mater. Chem. A*, 2014, **2**, 3092; (g) C.-H. Siu, L.T. L. Lee, P.-Y

Journal of Materials Chemistry A Accepted Manuscript

Ho, P. Majumdar, C.-L. Ho, T. Chen, J. Zhao, H. Lie and W.-Y. Wong, *J. Mater. Chem. C*, 2014, **2**, 7086; (h)Y. S. Yang, H. D. Kim, J.-H. Ryu, K. K. Kim, S. S. Park, K.-S. Ahn and J. H. Kim, *Synth. Met.*, 2011, **161**, 850; (i) H.-C. Chu, D. Sahu, Y.-C. Hsu, H. Padhy, D. Patra, J.-T. Lin, D. Bhattacharya, K.-L. Lu, K.-H. Wei and H.-C. Lin, *Dyes Pigm.*, 2012, **93**, 1488; (j) S. Ramkumar, S. Manoharan and S. Anandan, *Dyes Pigm.*, 2012, **94**, 503; (k) Y. Ooyama, N. Yamaguchi, I. Imae, K. Komaguchi, J. Ohshita and Y. Harima, *Chem. Commun.*, 2013, **49**, 2548; (l) S. S. Park, Y. S. Won,Y. C. Choi and J. H. Kim, *Energy Fuels*, 2009, **23**, 3732; (m) Cao, J. Peng, Y. Hong, X. Fang, L. Wang and H. Meier, *Org. Lett.*, 2011, **13**, 1610; (n) X. Ren, S. Jiang, M. Cha, G. Zhou and Z.-S. Wang, *Chem. Mater.*, 2012, **24**, 3493.

10 (a) Y. Liu, X. Wan, F. Wang , J. Zhou , G. Long , J. Tian and Y. Chen, *Adv. Mater.*, 2011, **23**, 5387; (b) S. C. Price, A. C. Stuart, L. Q. Yang , H. X. Zhou and W. You, *J. Am. Chem. Soc.*, 2011, **133**, 4625; (c) Y. Y. Liang, Z. Xu, J. B. Xia, S. T. Tsai, Y. Wu, G. Li, C. Ray and L. P. Yu, *Adv. Mater.*, 2010, **22**, E135; (d) H. X. Zhou, L. Q. Yang, A. C. Stuart, S. C. Price, S. B. Liu and W. You, *Angew. Chem. Int. Ed.*, 2011, **50**, 2995; (e) J. Zhou, X. Wan, Y. Liu, Y. Zuo, Z. Li, G. He, G. Long, W. Ni, C. Li, X. Su and Y. Chen, *J. Am. Chem. Soc.*, 2012, **134**, 16345;(f) J. Zhou, Y. Zuo, X.Wan, G. Long, Q. Zhang, W. Ni, Y. Liu, Z. Li, G. He, C. Li, B. Kan, M. Li and Y. Chen, *J. Am. Chem. Soc.*, 2013, **135**, 8484.

11 (a) P. Gao, H. N. Tsao, M. Grätzel and M. K. Nazeeruddin, *Org. Lett.*, 2012, **14**, 4330; (b) S. Jiang, X. Lu, G. Zhou and Z.-S. Wang, *Chem. Commun.,* 2013, **49**, 3899; (c) X. Hao, M. Liang, X. Cheng, X. Pian, Z. Sun and S. Xue, *Org. Lett.*, 2011, **13**, 5424; (d) Y.-R. Gao, L.-L. Chu, W. Guo and T.-L. Ma, *Chin. Chem. Lett.*, 2013, **24**, 149; (e) E. Longhi, A. Bossi, G. D. Carlo, S. Maiorana, F. D. Angelis, P. Salvatori, A. Petrozza, M. Binda, V. Roiati, P. R. Mussini, C. Baldoli and E. Licandro, *Eur. J. Org. Chem.*, 2013, 84; (f) Y.-Z. Lin, C.-W. Yeh, P.-T. Chou, M. Watanabe, Y.-H. Chang, Y. J. Chang and T. J. Chow, *Dye Pigm.*, 2014, **109**, 81.

12 H. Y. Chen, L. Lin, X. Y. Yu, K. Q. Qiu, X. Y. Lü, D. B. Kuang and C. Y. Su, *Electrochim. Acta.*, 2013, **92**, 117.

13 (a) H. Shang, Y. Luo, X. Guo, X. Huang, X. Zhan, K. Jiang and Q. Meng, *Dyes Pigm.*, 2010, **87**, 249; (b) S. Roquet, A. Cravino, P. Leriche, O. Alévêque, P. Frère and J. Roncali, *J. Am. Chem. Soc.*, 2006, **128**, 3459; (c) N. Zhou, L. Wang, D. W. Thompson and Y. Zhao, *Org. Lett.*, 2008, **10**, 3001; (d) Y. Lin, Z.-G. Zhang, Y. Li, D. Zhu and X. Zhan, *J. Mater. Chem. A*, 2013, **1**, 5128.

14 C. Y. Chen, H. C. Lu, C. G. Wu, J. G. Chen and K. C. Ho, *Adv. Funct. Mater.*, 2007, **17**, 29.

15 A. Hagfeldt and M. Grtäzel, *Chem. Rev.*, 1995, **95**, 49.

16 (a) J. Bisquert, *J. Phys. Chem. B.*, 2002, **106**, 325; (b) J. Bisquert, *Phys. Chem. Chem. Phys.*, 2003, **5**, 5360; (c) J. Bisquert, A. Zaban, M. Greenshtein and I. Mora-Sero, *J. Am. Chem. Soc.*, 2004, **126**, 13550; (d) Q. Wang, J. E. Moser and M. Grtäzel, *J. Phys. Chem. B*, 2005, **109**, 14945.

17 S. Kambe, S. Nakade, T. Kitamura, Y. Wada and S. Yanagida. *J. Phys. Chem. B*, 2002, **106**, 2967.

18 J.-H. Yum, D. P. Hagberg, S.-J. Moon, K. M. Karlsson, T. Marinado, L. Sun, A. Hagfeldt, M. K. Nazeeruddin and M. Grtäzel, *Angew. Chem. Int. Ed.*, 2009, **48**, 1576.

Journal of Materials Chemistry A Accepted Manuscript

Graphical abstract
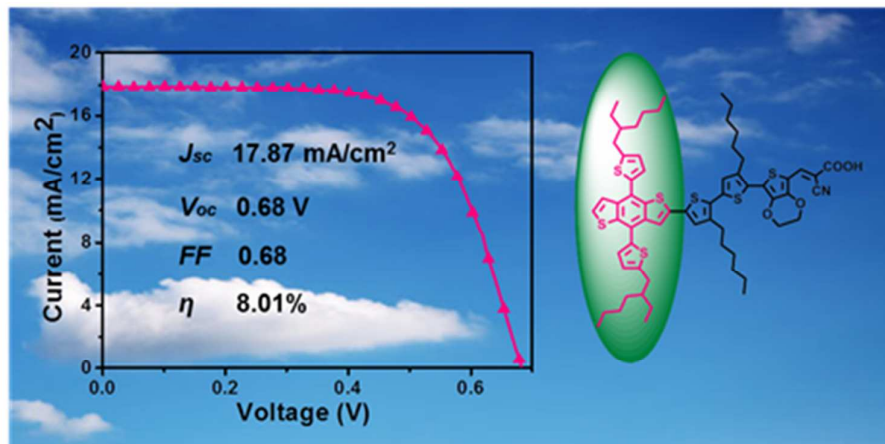
A stable sensitizer incorporating the benzo[1,2-b:4,5-b′]dithiophene donor was applied in DSSCs, showing the highest efficiency for amine-free organic dyes.